

# Magnetization and flux creep in thin $\text{YBa}_2\text{Cu}_3\text{O}_{7-\delta}$ films of various thickness

E. Sheriff,<sup>a)</sup> R. Prozorov, Y. Yeshurun, and A. Shaulov

*Institute for Superconductivity, Department of Physics, Bar-Ilan University, Ramat-Gan 52900, Israel*

G. Koren and C. Chabaud-Villard

*Department of Physics, The Technion, Haifa, Israel*

(Received 24 March 1997; accepted for publication 17 July 1997)

We report on the thickness dependence of the irreversible magnetization in superconducting  $\text{Y}_1\text{Ba}_2\text{Cu}_3\text{O}_{7-\delta}$  films of thickness 350–3000 Å. Our results reveal a nonmonotonous dependence of the persistent current density  $j$  on the film thickness, which is interpreted in terms of surface pinning and variations in the surface microstructure. Measurements of the time dependence of  $j$  show that under certain conditions relaxation curves of samples of different thickness cross each other, i.e., the sample with initially larger  $j$  exhibits after some time a lower  $j$ . The crossing point is shifted to shorter times as the temperature is increased. We propose a simple explanation to this effect and discuss its practical implications. Low dose heavy ion irradiation of the films has a modest effect on  $j$  and on the rate of its relaxation. © 1997 American Institute of Physics.

[S0021-8979(97)00321-6]

## I. INTRODUCTION

Significant advancements made in both theoretical understanding of high  $T_c$  superconductors (HTS) properties and in their fabrication techniques, promote the prospects of their future utilization in devices.<sup>1–3</sup> Attractive candidates for low power applications are thin superconducting films, which apart from well controlled fabrication techniques, have the advantage of relatively high critical current density, as compared to bulk specimen.<sup>4–10</sup> The film thickness is one of the important parameters that can be easily controlled and varied over a wide range. It is thus important to gain knowledge regarding the effects of thickness variation on the various physical properties of thin films.

In this paper we examine the thickness dependence of the magnetic properties of thin  $\text{YBa}_2\text{Cu}_3\text{O}_{7-\delta}$  (YBCO) films. Thickness variations may affect magnetic properties via different mechanisms, e.g., (1) Thickness dependence of the pinning force density resulting from surface pinning effects;<sup>5,6</sup> (2) Alteration of specimen microstructure with film thickness; (3) Changes in the ratio of film thickness to the characteristic length scales governing the magnetic properties of superconductors, e.g., the London penetration depth  $\lambda$  or the Larkin collective correlation length  $L$ .<sup>1,11</sup> In this work the significance of these mechanisms is examined on a series of laser ablated YBCO films of thickness ranging from 350 to 3000 Å.

The field and time dependence of the magnetic moment were measured for each sample at various temperatures. Our results reveal a non-monotonous dependence of the persistent current  $j$  on the film thickness:  $j$  increases sharply between 450 and 800 Å, peaks between 800 and 1000 Å, and then gradually decreases as the thickness is further increased. This behavior is interpreted as resulting from both surface-pinning effects and thickness dependent microstructural

variations. Measurements of the time dependence of magnetization reveal another intriguing phenomenon, namely the relaxation rates of thinner samples, with initially larger  $j$ , are larger than the relaxation rates of thicker samples, with initially lower  $j$ . This phenomenon leads, under certain conditions, to a crossing of the relaxation curves. The crossing point shifts towards shorter times as the temperature is increased. We propose a simple explanation to this effect and discuss its practical implications.

In addition to thickness variation one may affect the magnetic properties of films by irradiation. Numerous experiments in HTS crystals showed significant enhancement of the critical current density after irradiation.<sup>12</sup> However, irradiation results in HTS films are more ambiguous. Some works report current density enhancement following irradiation,<sup>13</sup> while others report on a reduction of the critical current as a consequence of irradiation.<sup>14</sup> So far, no systematic study of irradiation effects in films of different thickness has been reported. In order to examine the effects of heavy ion irradiation, two identical sets of YBCO films were prepared, one of which was irradiated with Pb ions. Our measurements show a modest increase of the persistent current of the irradiated samples throughout the applied field range 0–5 T. The relative increase, roughly temperature independent, is about 50% in the thinner samples and becomes smaller as the thickness is increased. A moderate thickness dependent irradiation effect is also noticed in magnetic relaxation measurements.

## II. EXPERIMENT

Two sets of  $\text{YBa}_2\text{Cu}_3\text{O}_{7-\delta}$  thin films of lateral dimensions 5 mm×5 mm and thicknesses 350, 450, 600, 800, 1000, 2000, and 3000 Å (quoted sample thickness is accurate to within  $\pm 5\%$ ) were prepared, using the laser ablation technique.<sup>15</sup> Thickness variation was achieved by gradual masking of the various samples during fabrication. This ensures uniformity of fabrication conditions for all samples.

<sup>a)</sup>Electronic mail: sheriff@physnet.ph.biu.ac.il

Films were deposited on a 150 Å layer of SrTiO<sub>3</sub> coating MgO (100) substrates. After the deposition, all films were coated with a 150 Å protective layer of SrTiO<sub>3</sub>, for prevention of rapid film degradation. Hence, the YBCO film is “sandwiched” between two thin SrTiO<sub>3</sub> layers. A pair of identical samples were prepared of each thickness, one of which was Pb irradiated prior to its measurement, while the other member of the pair was measured in its as-fabricated state. The irradiation dose was 10<sup>11</sup> ions/cm<sup>2</sup>, and the ion-beam energy was 5.8 GeV. Utilizing such energy level ensures the formation of linear amorphous tracks penetrating the sample. Irradiation was performed at GANIL, Caen.

Prior to the magnetic measurements described below, we measured the transition temperature  $T_c$  of all of the samples. Two different techniques were employed for that purpose to assure reliable results: (1) Low field cooling in a SQUID magnetometer; (2) microwave absorption. Both techniques gave similar results, showing the transition temperature to be  $86 \pm 0.5$  K. The width of the transition was approximately 1 K. Both  $T_c$  and the transition width show no significant variation for samples of different thickness. Moreover, irradiation does not seem to have any significant effect on  $T_c$  or on the transition width. A slight reduction (less than 0.5 K) in  $T_c$  was indeed noticed following irradiation. However, no particular thickness dependent effect of irradiation was noticed.

All magnetic measurements were conducted using a Quantum Design SQUID magnetometer. Sample orientation was such, that the external magnetic field was perpendicular to the film plane (i.e., along the  $c$  axis direction). A full (four quadrant) magnetization loop was taken at various temperatures between 5 and 75 K. Relaxation measurements were performed at a 0.2 T field. In all relaxation measurements the sample was zero-field-cooled to the desired temperature, then the external magnetic field was ramped up to 5 T, and subsequently lowered down to 0.2 T. Measurements of the persistent current were commenced 120 s after the field was stabilized at this level and continued, at each temperature, over a period of approximately 5 h. In addition, we performed several flux-in magnetic measurements, in which the field was elevated from  $-1$  to 0.2 T, then the rate of the magnetic moment change was examined. Flux-in and flux-out relaxation measurements at equal temperatures yielded similar results. Therefore, only the flux-out measurements are discussed.

The persistent current  $j$  was estimated by applying the Bean model<sup>16</sup> adapted for a square sample of lateral dimension  $a$  and thickness  $d$ :

$$j = \frac{30\Delta M}{da^3} \quad (1)$$

where the current density  $j$  is in A cm<sup>-2</sup>,  $\Delta M$  is in emu, and thickness  $d$  and lateral length  $a$  are in cm. The applicability of Eq. (1) has been experimentally verified for both films<sup>17</sup> and crystals.<sup>18</sup> Recent calculations of the critical state in thin films are also in agreement with this result.<sup>19</sup>

The above formula has also been used for the estimation of  $j$  from relaxation measurements. Since the magnetization

loops, for all samples and throughout the temperature range, are almost perfectly symmetrical with respect to the field axis, the value substituted for  $\Delta M$  was taken as double the measured magnetization value. The validity of this procedure is given further support, since our flux-in and flux-out measurements at equal temperatures yielded similar magnetization levels.

The surface morphology of the films was investigated using atomic force microscopy (AFM). All quoted values and reported features regarding morphology were deduced through utilization of picture analysis software, and are averages taken over an entire scan area of  $1 \mu\text{m} \times 1 \mu\text{m}$ .

### III. RESULTS

#### A. Microstructure

Typical results of AFM scans for films of 600, 1000, and 3000 Å are shown in Figs. 1(a), 1(b), and 1(c), respectively. As mentioned above, all samples were coated by a 150 Å layer of SrTiO<sub>3</sub>. As all samples bear an identical protective layer, any observed morphological variation between different samples thus has to be attributed to changes in the morphology of the superconducting film itself.

Our AFM study shows that the surface roughness depends on the sample thickness. In the lower thickness range a rapid change in the surface morphology is noticed. In the thinner samples ( $d < 800$ –1000 Å) an uneven grain-like structure with characteristic lateral variation of about  $\sim 150$ –200 Å and depth variation of  $\sim 50$ –100 Å is observed [Fig. 1(a)]. The characteristic length scale of this surface modulation increases, as film thickness is increased, up to an average lateral size of 400–600 Å and depth  $\sim 100$ –200 Å, for 1000 Å films [Fig. 1(b)]. For the thicker films, there is no apparent change in the sample surface morphology, which is clearly evident by comparing Fig. 1(b) with Fig. 1(c). Additionally, in the thinner films ( $d < 800$ –1000 Å) deep holes of  $\sim 40$  Å diameter, and linear density ranging from  $10^4$  to  $10^6$  holes/cm, penetrating through the film are observed. In the thicker samples ( $d \geq 1000$  Å) the deep holes disappear, and the granularity is reduced, as the average grain size increases. Similar thickness dependent surface morphology has also been observed in Refs. 5,6,20,21.

#### B. Magnetization loops

Figure 2 shows the magnetization curves of three films of different thickness at 40 K. Note that the width of the 3000 Å specimen magnetization loop is smaller than that of the 1000 Å specimen but larger than the width of the 450 Å one. This non-monotonous relation between the width of the loops and the sample thickness is observed at different temperatures and fields for both sample sets. Translating the width of the loop to the persistent current, using Eq. (1), one obtains the results shown in Fig. 3 for different temperatures and an applied field of 0.2 T. Figure 4 shows the persistent current at various fields at a temperature of 10 K. In both cases  $j$  increases rapidly, between about 450 and 800 Å. A more moderate increase of  $j$  is observed between 800 and 1000 Å. Above this thickness the persistent current gradually

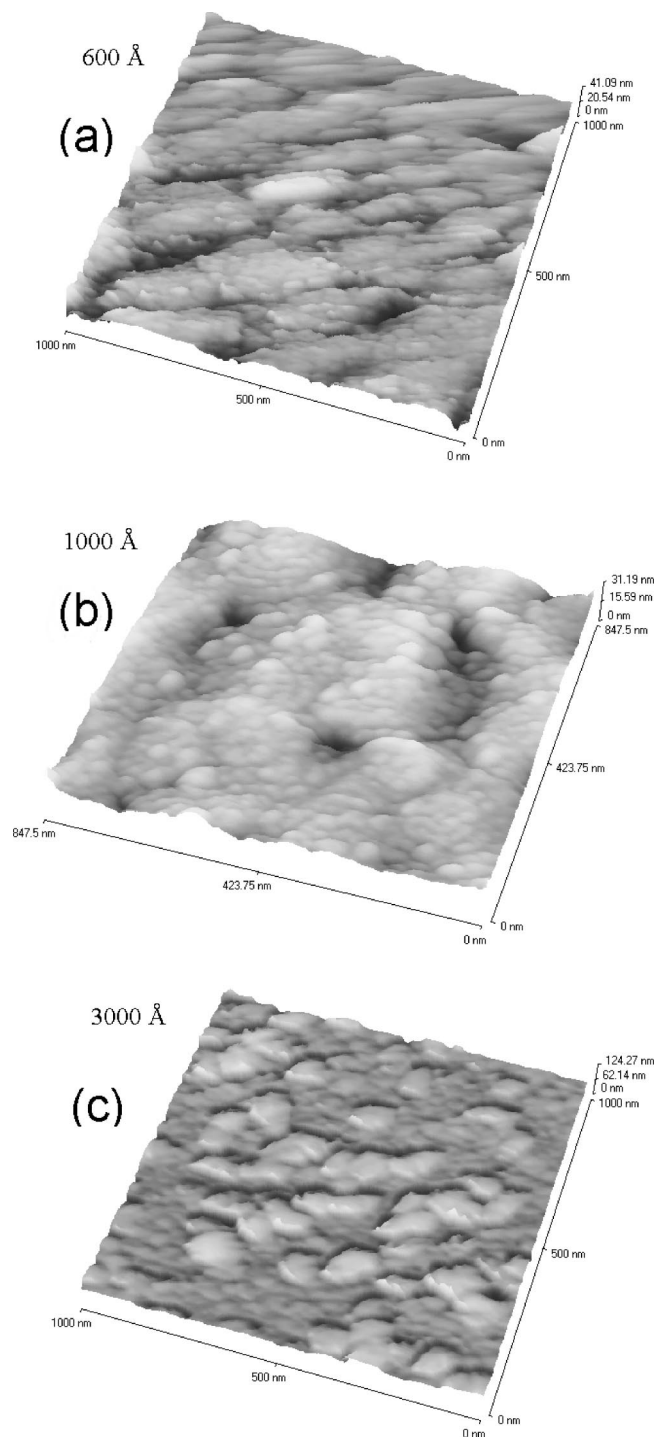


FIG. 1. Atomic force microscopy figures showing surface morphology of (a) 600 Å, (b) 1000 Å, and (c) 3000 Å samples.

decreases. Figures 3 and 4 clearly show that the applied field intensity and the temperature have but a minor effect on the shape of the  $j$  versus thickness curves. In particular, the position of the peak remains unaltered under either temperature or field change. We emphasize that the peculiar shape of the curves in Figs. 3 and 4 is not an artifact of the technique utilized to derive the persistent current, rather it is an inherent feature of the “raw” magnetization data.

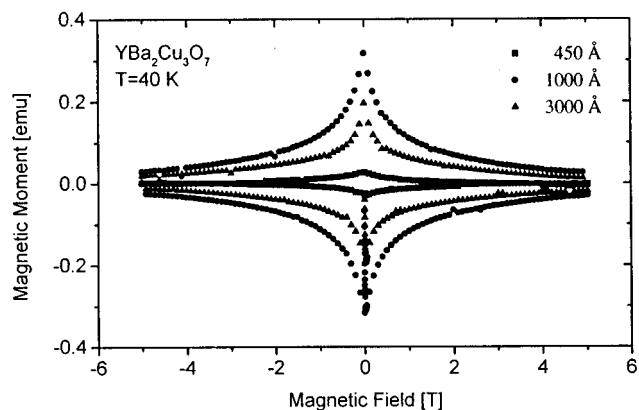


FIG. 2. Magnetization loops at 40 K of 450 Å, 1000 Å, and 3000 Å samples.

### C. Relaxation

Figure 5 shows typical relaxation data, i.e.,  $\Delta M$  versus  $\ln(t)$  (where  $\Delta M$  is double the measured remanent magnetization) of one of the films (800 Å), normalized by the initial magnetization level at the beginning of the measurement, at different temperatures between 5 K and 75 K. Plotted on a semi-logarithmic scale, the curves are approximately linear at lower temperatures, while at higher temperatures the curves become nonlinear, and the difference in relaxation rates becomes more prominent.

Figures 6(a) and 6(b) compare data of  $\Delta M$  versus time for 600 and 3000 Å samples at 10, 40, 60, and 70 K. At low temperatures, e.g., 10 K, the magnetization level of the 3000 Å specimen is higher than that of the 600 Å specimen for the entire measurement time window. However, as the temperature is increased from 10 to 40 K, the change in  $\Delta M$  in the 3000 Å sample is more significant than for the 600 Å sample. Eventually, just below 40 K, the two curves switch positions [Fig. 6(a)]. As the temperature is further increased, yet another phenomenon becomes evident. Whereas the initial magnetization level of the thicker specimen is more temperature-sensitive than that of the thinner one, the situation is inverted when it comes to the time derivative of the magnetization, i.e., the relaxation rate. At 10 K the relaxation

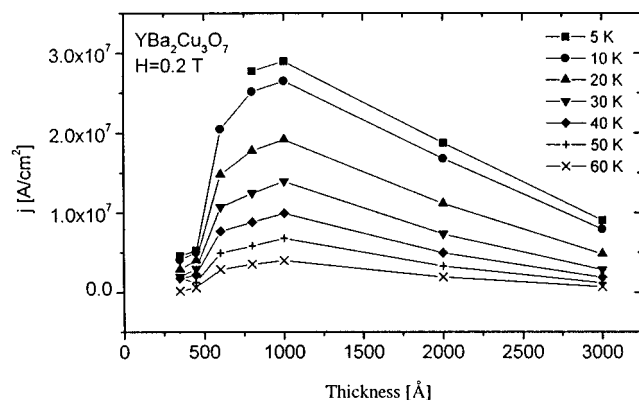


FIG. 3. Persistent current plotted vs thickness, at 0.2 T applied field, for various temperatures, between 5 K and 60 K. Lines are guide for the eye.

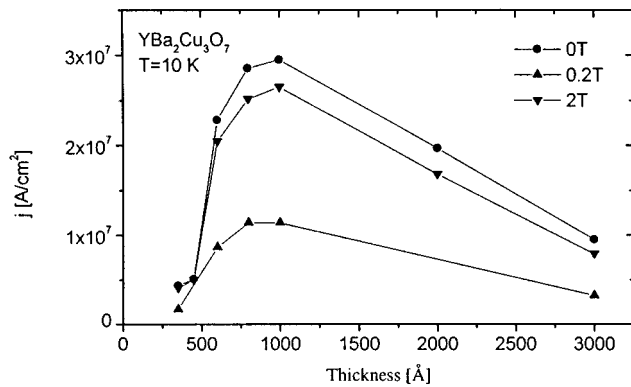


FIG. 4. Persistent current plotted vs thickness at 10 K and 0.2 T, 1 T, and 2 T applied field. Lines are guide for the eye.

rate of the thinner specimen is somewhat lower than that of the thicker one. At 40 K the relaxation rates of the two samples become approximately similar [Fig. 6(a)]. With further temperature increase the relaxation rate of the thinner sample becomes such, that at about 60 K after some relaxation has occurred the two relaxation curves cross each other [Fig. 6(b)]. Further temperature increase shifts the intersection of the relaxation curves towards shorter times. At 70 K the intersection of the relaxation curves seems to occur prior to the beginning of our time window [Fig. 6(b)]. It is therefore evident that the magnetic field relaxation rate as well as its temperature dependence are thickness dependent.

Note, that despite the crossing of relaxation curves for samples of different thickness at elevated temperatures, the general features of the thickness dependence of the persistent current, as shown in Fig. 3, are maintained. This is demonstrated in Fig. 7, which depicts the persistent current as a function of thickness, at various times. Specifically, the position of the peak is maintained throughout our measurement time.

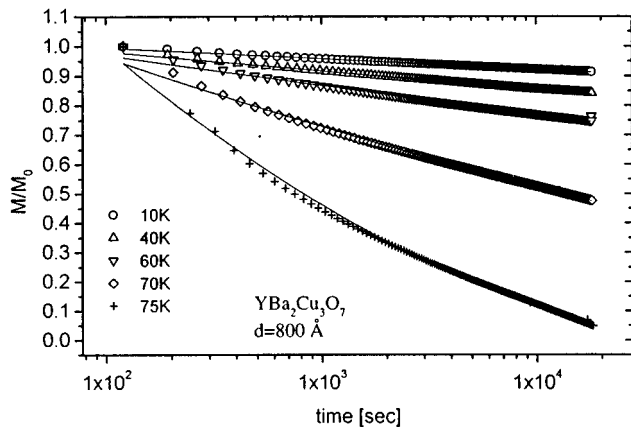
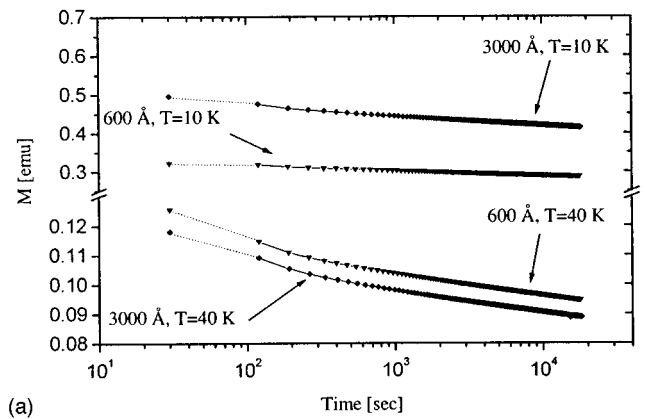
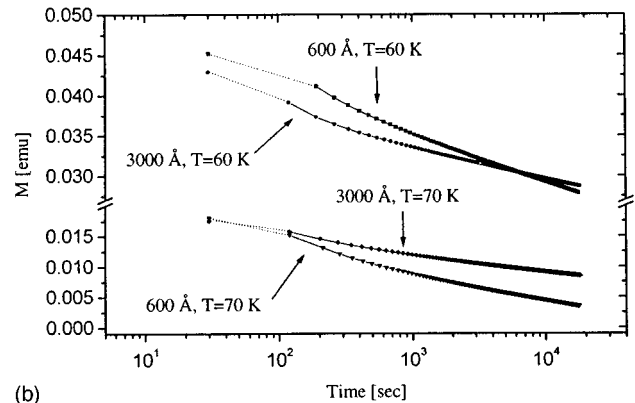


FIG. 5. Magnetization of an 800 Å sample, normalized by the initial magnetization level at the beginning of the measurement, plotted vs time, at various temperatures between 5 K and 75 K. Lines are theoretical fits to Eq. (3).



(a)



(b)

FIG. 6. Magnetization vs time. Comparison of 600 Å and 3000 Å samples, at 10 K and 40 K (a), and 60 K and 70 K (b). The first data point on each of the curves was taken from magnetization loops measurements (in which the magnetization was measured approximately 30 s after the required field level had been reached).

#### D. Irradiation effects

A moderate increase of approximately 50% in the persistent current of irradiated samples, as compared to their identical unirradiated sample, was observed. Figure 8 compares the persistent current versus field at temperatures 5, 50, and 70 K, of unirradiated and irradiated samples of 800 Å thickness. As expected, as the temperature is increased, the magnetization levels of both irradiated and unirradiated

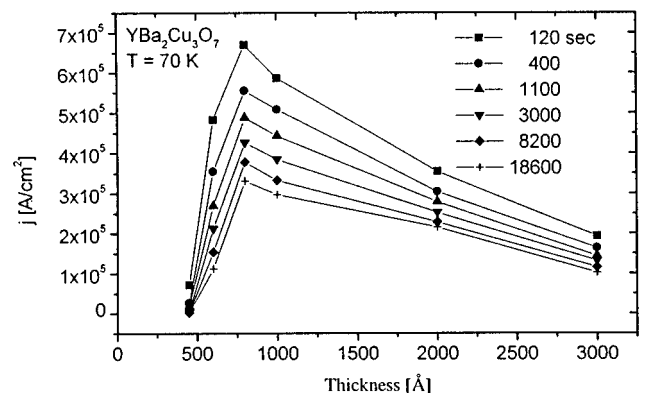


FIG. 7. Persistent current, at 70 K extracted from relaxation measurements data, plotted vs thickness, at different times. Lines are guide for the eye.

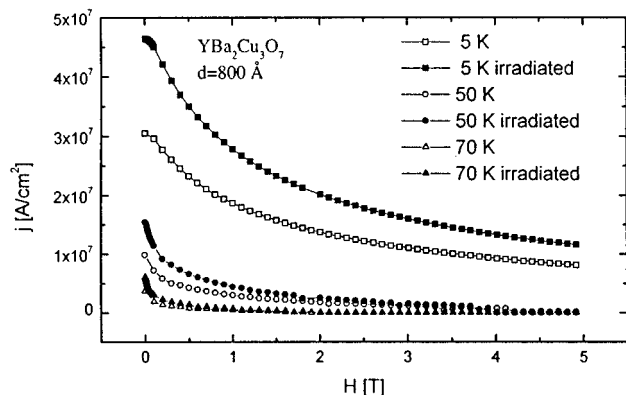
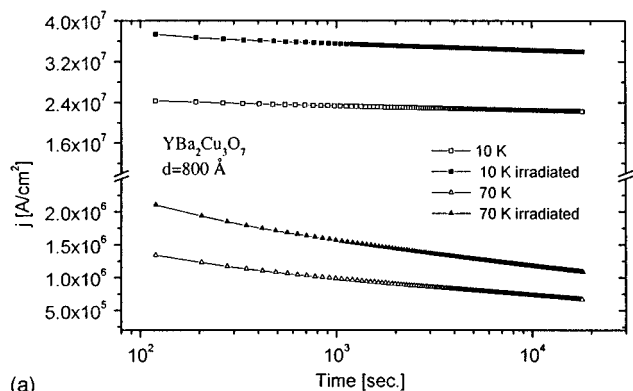


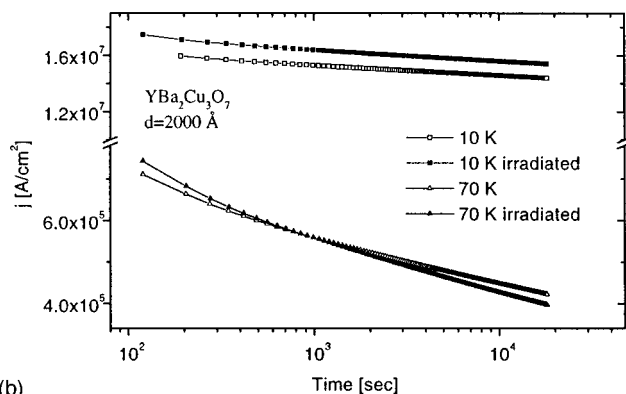
FIG. 8. Persistent current vs magnetic field of irradiated and unirradiated 800 Å samples, at 5 K, 50 K, and 70 K.

samples drop. However, the relative increase of  $j$  in the irradiated samples remains approximately constant throughout the temperature range (5–75 K), and field range (0–5 T). We therefore assert that low-dose irradiation moderately enhances the persistent current density of thin superconducting films. However, this effect is minute in comparison to the effect of heavy ion irradiation in HTS single crystals.<sup>12</sup>

A moderate effect of heavy ion irradiation is also noticed in relaxation measurements. Figures 9(a) and 9(b) compare relaxation data of irradiated and unirradiated samples of thickness 800 and 2000 Å, respectively, at temperatures 10 and 70 K. One notices that at low temperatures irradiated and



(a)



(b)

FIG. 9. Persistent current vs time of irradiated and unirradiated samples, 10 K and 70 K. (a) 800 Å samples; (b) 2000 Å samples.

unirradiated samples of the same thickness have quite similar decay rates. At elevated temperatures, irradiated samples incline toward higher relaxation rates than equal thickness unirradiated ones. Comparison between Figs. 9(a) and 9(b) readily shows that irradiation leads to more significant changes in current magnitude in thinner samples. For thicker samples, as irradiation scarcely increases the current density, the higher relaxation rates of the irradiated samples may lead to crossing of the relaxation curves. Consequently, irradiated samples having initially slightly higher current densities, relax in such a manner that after some relaxation they have lower current densities than unirradiated samples of the same thickness.

## IV. DISCUSSION

### A. Current density versus thickness

In this section we discuss the nonmonotonous thickness dependence of the persistent current. Specifically, the rather sharp increase of the persistent current between 450 Å and 800–1000 Å, and the gradual decrease of the current on a further thickness increase.

In earlier works,<sup>4–9,11</sup> observations of current variations with sample thickness were associated with the ratio of sample thickness and basic characteristic length scales such as the Larkin correlation length  $L(T, t)$  or the penetration length  $\lambda(T)$ . We argue that in our case, the observed increase of  $j$  in the thickness range up to approximately  $d_p \approx 800$ –1000 Å is unlikely to be related to this effect. Note, that all  $j$  versus thickness curves in Fig. 3 exhibit the same features regardless of temperature, and that the main difference between the various isochamps is the magnitude of  $j$ . In particular, the persistent current attains a maximum at the same thickness  $d_p$ , throughout the temperature range 5–60 K. Thus, the ratio between film thickness and characteristic superconducting length scales cannot be relevant in our case, as these length scales are strongly temperature dependent. Also, concerning the collective correlation length  $L$ , a crossover from a 2D pinning (at small thickness, i.e.,  $d < 2L$ ) to a 3D pinning (at larger thickness, i.e.,  $d > 2L$ ) is expected at  $d \approx 2L$ .<sup>11</sup> So one is tempted to interpret a sharp change in  $j$  vs  $d$  as due to such a crossover. However, this would lead to conclusions that contradict our experimental results. In the 2D pinning regime we have to use  $d$  instead of  $L$  as the relevant correlation length. Since  $j \propto 1/L$  we should expect a decrease of  $j$  with an increase of thickness before the peak (in a 2D regime), while our experimental results show an increase of  $j$  with thickness.

We therefore propose an explanation that attributes the observed increase of  $j$  to changes in the surface morphology. This assertion is supported by our AFM studies. Examining the method utilized to derive  $j$ , i.e., the Bean model, while taking into consideration our AFM observations, the rapid increase of  $j$  may be quite straightforwardly explained. The Bean model, Eq. (1), assumes a uniform current density throughout the sample cross section. Denoting  $I$ , the total current flowing through the entire sample cross-section  $S = d \cdot a/2$ , the estimated current density is thus  $j = I/S$ . However, as our AFM studies indicate, the thinner samples, up to

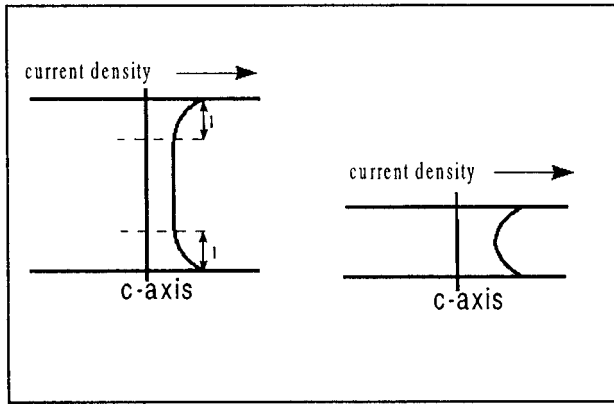


FIG. 10. Schematic description of the current density profile (along the  $c$  axis), of samples of thickness lower than  $2l$  and samples of thickness larger than  $2l$ .

a thickness of approximately  $d_p$ , contain a large amount of penetrating holes. Therefore, in practice the current flows through a smaller cross-section  $S_e \leq S$ . The “real” current density within the sample should be estimated as  $j_r = I/S_e$ , thus, current estimated from Eq. (1) is  $j = [S_e(d)/S(d)]j_r$ . Our AFM studies show a rapid decline in the number of penetrating holes with thickness increase, up to around  $d_p$ . This implies that  $S_e$ , rapidly increases up to that thickness. Consequently,  $j$  is expected to increase in this thickness range. This simple interpretation implies that the peak position is temperature independent, as it is related solely to the sample morphology.

Next, we consider the gradual decrease of  $j$  for thicknesses greater than  $d_p$ . At this thickness range there are no penetrating holes through the films, and the morphology becomes approximately thickness independent. Our interpretation of the data in this range is therefore based on a concept conceived by McElfresh *et al.*<sup>5</sup> who have suggested that the magnetic flux pinning in thin samples results from both surface and bulk pinning. The gradual decrease of the persistent current with thickness (Figs. 3 and 4) may be readily interpreted in terms of this simple model. Assuming that the pinning force is larger on the surface than within the bulk, the persistent current density is larger on the sample surface, gradually decreasing away from the surface, until it reaches a limiting value  $j_b$ , at a distance  $l$  away from the surface,  $l$  being smaller than the London penetration depth  $\lambda$  (for a detailed discussion see Ref. 10). Figure 10 schematically compares current profiles along the  $c$  axis, for thin and thick samples. In the thinner samples the current does not have the required thickness to become fully attenuated to the level of the bulk current density  $j_b$ , consequently the minimal current density along the  $c$  axis is larger in samples of thickness  $d < 2l$  compared with thicker samples of thickness  $d \geq 2l$ . Assuming, for simplicity (for more accurate discussion see Ref. 10), that  $j = j_s(1 - z/l) + j_b z/l$  where  $j_s$  is the current density on the surface we obtain for the average current density  $\bar{j}$ :

$$\bar{j} = j_s - \frac{d}{4l}(j_s - j_b) \quad 2l \geq d$$

$$\bar{j} = j_b + \frac{l}{d}(j_s - j_b) \quad 2l \leq d. \quad (2)$$

In both cases, it is readily seen that the average persistent current density decreases with an increase of thickness — first linearly and then as  $1/d$ . This prediction for a reduction of the persistent current is qualitatively confirmed by the experiment. Unfortunately, our data are too sparse to allow quantitative verification of this prediction. However, other works that investigated the thickness dependence of the current density show data supportive of the above model. For example, Joos *et al.*<sup>6</sup> observe a rather linear attenuation of the current density with increase of thickness, for YBCO films of 3000–7000 Å while Bhattacharya *et al.*<sup>7</sup> in their investigation of thicker YBCO films of 10 000–80 000 Å obtain a nonlinear attenuation of the current density with thickness, resembling the expected  $1/d$  behavior.

## B. Magnetic relaxation

At temperatures below 60 K our relaxation measurements yield quite ordinary results, namely, the relaxation is logarithmic in time, and the relaxation rates of samples of different thickness, are rather similar. However, at temperatures above 60 K an anomalous and intriguing phenomenon is evident. At these higher temperatures the relaxation rates of the thinner samples become evidently larger than the relaxation rates of thicker samples. This phenomenon leads to crossing of some of the relaxation curves, as the initial current density is larger in thinner films [Fig. 6(b)]. This crossing is evident in the magnetization versus time curves (as shown) as well as in the current density versus time curves, not presented here. The simple phenomenological interpretation of this effect is straightforward. The relaxation curves shown in Fig. 5 can be well described by the expression:

$$j(t) = j_c \left( 1 - \frac{kT}{U_c} \ln(t/t_0) \right)^{1/\beta}, \quad (3)$$

which corresponds to a general dependence of the activation energy  $U$  on the current density  $j$ :

$$U(j) = U_c \left[ 1 - \left( \frac{j}{j_c} \right)^\beta \right].$$

The solid curves in Fig. 5 show reasonably good fits of Eq. (3) to the data with  $\beta = 4/7$  for all temperatures. From Eq. (3) it follows that the relaxation curves of two films of thickness  $d_1$  and  $d_2$  ( $d_1 < d_2$ ), characterized by critical current densities  $j_c^1$  and  $j_c^2$  ( $j_c^1 > j_c^2$ ), and effective activation energies  $U_c^1$  and  $U_c^2$  ( $U_c^1 < U_c^2$ ), cross each other at time  $t_c$  given by:

$$t_c = t_0 e^{(1-A)/B}, \quad (4)$$

where  $A = (j_c^2/j_c^1)^\beta$  and  $B = 1/U_c^1 - A/U_c^2$ . Equation (4) readily shows that the time at which two relaxation curves cross each other increases exponentially as the temperature decreases. This explains why crossing of relaxation curves is normally observed at elevated temperatures. It should be noted that this phenomenon is not unique to relaxation

curves described by Eq. (3). A similar expression for  $t_c$  [Eq. (4)] can be obtained for relaxation curves described by the “interpolation formula”<sup>3</sup>  $j(t) = j_c / [1 + \mu k T / U_c \ln(t/t_0)]^{1/\mu}$ .

## V. CONCLUSIONS

Our measurements on laser ablated YBCO films of thickness 350–3000 Å show that their magnetic properties are affected by both surface pinning and thickness dependent film morphology. As the thickness is decreased, domination of the surface pinning mechanism over the bulk pinning gives rise to increasing critical current density  $j_c$ . At low temperatures, larger  $j_c$  implies larger persistent current density  $j$  over a reasonably long time range. The reduction in  $j$  observed in our measurements as the thickness is decreased below 800–1000 Å is a direct consequence of sharp variations in the microstructure of the films. In general, larger  $j_c$  does not imply larger persistent current, as the relaxation curves cross each other. The crossing of the relaxation curves occurs at shorter times as the temperature is increased. Heavy-ion irradiation has a modest effect on  $j$  and magnetic relaxation in films.

Our results contain significant implications related to application of thin superconducting films. For applications of films at low temperatures, thinner films with larger  $j_c$  and  $j$  are preferable. However, for applications at relatively high temperatures, crossing of the relaxation curves dictates consideration of the characteristic time window of the experiment or application. For dc applications, thicker films are preferable due to their lower relaxation rates. However, for ac applications in which relaxation effects are less significant, one may wish to use thinner films in order to gain higher persistent currents.

## ACKNOWLEDGMENTS

We acknowledge helpful discussions with E. Sonin and thank M. Konczykowski and S. Bouffard for the irradiation at GANIL, Caen (France). This research was supported in part by the Israel Science Foundation and by the Heinrich Hertz Minerva Center for High Temperature Superconductivity.

Y.Y. acknowledges support from the USA–Israel Binational Science Foundation. R.P. acknowledges support from the Clore Foundations. A.S. acknowledges support from the France–Israel Cooperation Program AFIRST.

- <sup>1</sup>G. Blatter, M. V. Feigelman, V. B. Geshkenbein, A. I. Larkin, and V. M. Vinokur, *Rev. Mod. Phys.* **66**, 1125 (1994).
- <sup>2</sup>E. H. Brandt, *Rep. Prog. Phys.* **58**, 1465 (1995).
- <sup>3</sup>Y. Yeshurun, A. P. Malozemoff, and A. Shaulov, *Rev. Mod. Phys.* **68**, 911 (1996).
- <sup>4</sup>L. Civale, T. K. Worthington, and A. Gupta, *Phys. Rev. B* **43**, 5425 (1991).
- <sup>5</sup>M. McElfresh, T. G. Miller, D. M. Schaefer, R. Reifenberger, R. E. Muenchausen, M. Hawley, S. R. Foltyn, and X. D. Wu, *J. Appl. Phys.* **71**, 5099 (1992).
- <sup>6</sup>C. Jooss, A. Forkl, R. Warthmann, H.-U. Habermeier, B. Leibold, and H. Kronmüller, *Physica C* **266**, 235 (1996).
- <sup>7</sup>D. Bhattacharia, P. Choudhury, S. N. Roy, and H. S. Maiti, *J. Appl. Phys.* **76**, 1120 (1994).
- <sup>8</sup>A. Neminsky, J. Dumas, B. P. Thrane, C. Schlenker, H. Karl, and B. Stritzker, *Phys. Rev. B* **50**, 3307 (1994).
- <sup>9</sup>H. Wen, H. G. Schnack, R. Griessen, B. Dam, and J. Rector, *Physica C* **241**, 352 (1994).
- <sup>10</sup>R. Prozorov, E. B. Sonin, E. Sheriff, Y. Yeshurun, and A. Shaulov (unpublished).
- <sup>11</sup>E. H. Brandt, *J. Low Temp. Phys.* **64**, 375 (1986); P. H. Kes and R. Wordenweber, *J. Low Temp. Phys.* **67**, 1 (1987).
- <sup>12</sup>See, for example, M. Konczykowski *et al.*, *Phys. Rev. B* **44**, 7167 (1991); L. Civale *et al.*, *Phys. Rev. Lett.* **63**, 648 (1991).
- <sup>13</sup>W. Schindler *et al.*, *Supercond. Sci. Technol.* **5**, S129 (1992).
- <sup>14</sup>S. K. Agarwal, O. Muller, J. Schubert, and C. Schlenker, *Physica C* **180**, 203 (1991).
- <sup>15</sup>G. Koren, E. Polturak, B. Fisher, D. Cohen, and G. Kimel, *Appl. Phys. Lett.* **50**, 2330 (1988).
- <sup>16</sup>C. P. Bean, *Phys. Rev. Lett.* **8**, 250 (1962).
- <sup>17</sup>B. Oh, M. Naito, S. Aronson, P. Rosenthal, R. Barton, M. R. Beasley, T. H. Geballe, R. H. Hammond, and A. Kapitulnik, *Appl. Phys. Lett.* **51**, 852 (1987).
- <sup>18</sup>Y. Yeshurun, M. W. McElfresh, A. P. Malozemoff, J. Haghorst-Trewhella, J. Mannhart, F. Holtzberg, and G. V. Chandrashekar, *Phys. Rev. B* **42**, 6322 (1990).
- <sup>19</sup>E. H. Brandt and M. V. Indenbom, *Phys. Rev. B* **48**, 12893 (1993); E. Zeldov, J. R. Clem, M. McElfresh, and M. Darwin, *Phys. Rev. B* **49**, 9802 (1994).
- <sup>20</sup>Y. Chen, L. M. Wang, H. C. Yang, H. E. Horng, and H. H. Sung, *Physica C* **255**, 30 (1995).
- <sup>21</sup>J. Summhammer, K. Kundzins, G. Samadi Hosseinali, R. M. Schalk, H. W. Weber, S. Proyer, E. Stangl, and D. Bauerle, *Physica C* **242**, 127 (1995).